DENSITY FUNCTIONAL STUDY ON THE STABILITY AND REACTIVITY OF Pt(100) AND Pt(111) SURFACES MODIFIED BY Ni ATOMS

M. B. López[1],   E. A. Castro[2]*

[1] Centro de Investigaciones Fisicoquímicas, Teóricas y Aplicadas (CIFTA), Facultad de Ciencias Exactas y Naturales, Universidad Nacional de Catamarca, Avda. Belgrano 300, Catamarca 4700, Argentina.

[2] INIFTA, Theoretical Chemistry Division, Suc.4, C.C. 16, La Plata 1900, Buenos Aires, Argentina

ABSTRACT

DFT study on the the stability and reactivity of Pt(100) and Pt(111) surfaces modified by nickel UPD monolayer deposition have been carried out. We used the binding energy calculation of bimetallic structures versus the cohesion energy of the bulk adsorbate to quantify the underpotential shift (Eupd) to determine the stability of the bimetallic systems. The reactivity of the clean and modified surface was analized by energy levels of the highest occupied molecular orbital (HOMO), softness and local softness. We concluded that the stability of Pt(100)$_{25}$Ni$_9$ and Pt(111)$_{25}$Ni$_{10}$ bimetallic structures cannot be explained by excess of the metal- substrate binding energy but the instability can be explained by structural effects. We found that the modified surfaces are more reactive and the active sites are located in the centre of the cluster which favors the formation of islands of atoms onto these surfaces.

* Corresponding author (eacast@gmail.com, castro@quimica.unlp.edu.ar)

1-INTRODUCTION

The anomalous behaviour of small amounts of metals electrodeposited on foreign metal substrate have been known for a very long time [1,2]. The anomaly is the apparent violation of Nernst´s law, that is, a part of metal electrodeposited on foreign metals surfaces is oxidized a much more positive potential than the reversible Nernst potential in the same electrolite. Later, the potential difference between the oxidation potential of metal deposited on "inert" foreign metal substrate and the reversible Nerst potential of the depositing metal in the same electrolite was called underpotential shift (Eupd) an the process itself underpotential de position (UPD) [3,4].

This apparent violation of Nernst´s law simply reflects the fact that the bond between metal and substrate is stronger than that between the adatoms of the deposited metal and hence the deposit spreads over the substrate [4].

It has been found that a linear correlation of unit slope exists between Eupd and the difference between the work function ( ) of the support (substrate) and that of the bulk metal overlayer [5]. This finding, predicted theoretically [6], is compatible with a model of ionic bond formation between the first metal atom deposited and the foreign substrate, although alternative explanations have been offered. As coverage increases, lateral interactions reduce the adsorption strength and this can be taken as an indicator that ionic bond is gradually converted to metallic bond at full coverage.

The simple correlation between Eupd and has been observed with polycristalline metal surfaces [5]. The same correlation should be expected with single crystal faces:

metal deposition should begin at a more positive potential on the faces with higher work function ( ), ie, on the more compact face. However no definite experimental confirmation can be observed in this case.

The underpotential deposition of bimetallic systems like Pt/Ag, Pt/Cu and Pt/Au has been widely studied [7], nevertheless there exist other systems like Pt/Ni of which there is not much experimental information because nickel electrodeposits on Pt are produced in the potential range where the hydrogen evolution reaction takes place.

The underpotential deposition (UPD) of Ni on pollycristalline Platinum was reported by different authors [8-12] and recentlty, Chatenet et al. [13] have evaluated such phenomenon on platinum single crystal in sulphuric media using cyclic voltammetry. This study described the possibility for nickel underpotential deposition on Pt(110) and Pt(111) electrode surfaces. At low pH values (pH≈1), nickel UPD peaks overlap with the hydrogen adsorption/desorption region which renders difficult any coverage estimation. At higher pH(pH≈ 2-3) the overlapping is less severe, nickel coverage increases, which never exceeds a full monolayer, and can be estimated. In these conditions Ni-UPD occurs on reconstructed Pt(110) surfaces, probably for structural reasons. Nickel submonolayer on Pt(110) exhibits remarkable properties for CO oxidation. No nickel-UPD was detected on Pt(111) in sulphuric acid solution

Since the mechanism of nickel-UPD on platinum is extremely complex due to the co-adsorption of anions and hydrogen a theoretical study result interesting, starting off from a simple model, about the different aspects that can favor the occurrence of this phenomenon. One more a finished idea on structural and energetic aspects involved the nickel-upd can contribute to the understanding of this phenomenon.

The present work refers to DFT calculations for describing the stability and reactivity of Pt(100) and Pt(111) surfaces modified by nickel UPD monolayer deposition. We have considered two model systems: i)a clean platinum surface ii)modified platinum surface adsorbing a metallic atom.

Changes in the work function of Pt (100) and Pt (111) induced by the adsorption of metallic ad-atoms allow to analyzing the interaction adsorbato-sustrato. The binding energy calculation of bimetallic structures versus the cohesion energy of the bulk adsorbate allows to quantize the underpotential shift (Eupd) and to determine the stability of the bimetallic systems: $Pt(100)_n Ni_m$, $Pt(111)_n Ni_l$ (n = 25, m = 9 and l = 10).

The reactivity of the clean and modified surfaces were analized by: i)energy levels of the highest occupied molecular orbital (HOMO), ii)sofness and local softness.

2-METHODOLOGY

Density function theory (DFT) as implemented in Gaussian 03 [14] has been used for all the calculations. The hybrid B3LYP density functional method was used, which includes Becke´s 3-parameter nonlocal-exchange functional [15] with the correlation functional of Lee et al [16]. The effective-core-potential LANL2DZ basis set [17] is used for the atomos of Ni and Pt.

The Pt single crystal electrodes with (100) and (111) surfaces were modeled using $Pt(100)_{25}$ and $Pt(111)_{25}$ clusters. Both clusters were built with 16 atoms in the first layer and 9 atoms in the second layer, Fig. 1.a y b.

In order to simulate the atom deposition of Ni on (100) and (111) crystalline planes the Pt surface is covered with with nine and ten atoms, respectively, Figure 1 c and d.

In adsorption phenomena, the coordination of an adsorbate may involve mainly one, two or more metallic atoms and according to this choice we can considerer three adsorption sites:a) on-top site (lineal or monocoordinate), b) bridge site (bicoordinate) and c) hollow site (largest coordinate site). For the platinum (100) plane the three different sites have been recognized (tetraccordinate only if surface shell is considered), as shown in Fig. 2.

For the Pt(111) surface besides the on top and bridge sites there were recognized two hollow sites: hollow(3-3) and hollow(3-1), according to the location of the atoms within the second shell at the largest coordination site, as shown in Fig. 3.

Nearest neighbor distances (lattice constants) $d_{Pt-Pt} = 0,277$ nm and $d_{Ni-Ni} = 0.25$ nm were taken from X-ray difraction study [18]. The Pt-Ni distance was taken as 0.263 nm (average distance: $(d_{Pt-Pt}+d_{Ni-Ni})/2$).

The optimization of the geometry of the metallic ad-atoms was carried out maintaining fixed the geometry of the susbstrate. This optimization allows to predict the adsorbate structural changes when ni atoms interacting with the surface Pt (100) and Pt (111).

Atomic populations were calculated using Mulliken population analysis, moreover, we used the electron density condensed to the atom to analize the population distribution. This value between different atoms is indicating stronger bonds between these atoms.

2-a-Underpotential shift

Underpotential deposition (UPD) of metals is an electroreduction of metallic ions on foreign metal susbstrate (S) in the underpotential range (Eupd), that is, in a potential region positive to the Nernst potential of the depositing M^{z+}/M couple [19]:

$$\Delta Eupd = E_{ads} - E_N \geq 0 \qquad (1)$$

The reason for the underpotential deposition is the excess binding energy of an adsorbed metal atom on a foreign metal surface (E_{S-Mads}) relative to the binding energy of a deposited metal atom on a surface of its own kind (E_{M-Mads}):

$$E_{S-Mads} \geq E_{M-Mads} \qquad (2)$$

In the present work the binding energy E_{S-Mads} and E_{M-Mads} where obtained as:

$$E_{S-Mads} = E_{clusterPt/M} - E_{clusterP}t - E_M \qquad (3)$$

$$E_{M-Mads} = E_{clusterM/M} - E_{clusterM} - E_M \qquad (4)$$

Where $E_{clusterPt/M}$ is the energy of metallic monolayer adsorbed on Pt surface, $E_{clusterPt}$ is the Platinum cluster energy , E_M is the monolayer energy, $E_{clusterM/M}$ is the energy of metalic monolayer (M) adsorbed on cluster of it own kind (cluster M), $E_{clusterM}$ is the cluster M energy, respectively.

The underpotential shift can be calculated by the following relationship

$$Eupd \approx E_{S\text{-}Mads} - E_{M\text{-}Mads} \quad (5)$$

According to this definition underpotential deposition (UPD) happens when $E_{S\text{-}Mads}$ is greater than the $E_{M\text{-}Mads}$.

In this model the adsorption anion and solvent effects are not considered, they can play an important rol in the stabilization or destabilization of the adsorbed monolayer.

2-b-Reactivity Indicators

DFT has provided a very useful framework for the theoretical description of charge distribution and related properties, such as the chemical reactivity of chemical compounds. Well-known chemical concepts, e.g. electronegativity, chemical potential, ionization potential, electron affinity, hardness and sofness, all emerge from DFT calculations. Hardness and softness were defined as global reactivity indicators, and helped to justify Sanderson´s electronegativity equalization principles [20], Pearson´s hard-soft acid.base (HSAB) principle [21], and the maximun hardness principle [22,23]. In this study, we use the softness to represent the global reactivity of the surface. The softness can be defined [24] as the inverse of the hardness, [25] as

$$S = \frac{1}{2} = \left(\frac{\partial N}{\partial} \right)_{v(r)} \quad (6)$$

Where is the electronic chemical potential, which is identified with the negative of electronegativity, [26] as

$$= \left(\frac{\partial E}{\partial N} \right)_{v(r)} = - \qquad (7)$$

And E is the energy, N is the number of electrons of the systems, and v*(r)* is the external potential. S can be represented, by a finite difference approximation as follows [21],

$$S = \frac{1}{IP - EA} \qquad (8)$$

Where IP and EA are the vertical ionization potential and electron affinity, respectively.

$$IP = E(N-1)-E(N) \qquad (9)$$

$$EA = E(N)-E(N+1)$$

Form DFT, local descriptor, such as hardness and softness kernels [27, 28], local hardness [24], local softness [24] and Fukui function indices [29], were derived to explain the reactivity or selectivity at a particular site of the system. In this work, we adopted the local softness to describe the local reactivity of the surfaces. The local softness is defined as

$$s(r) = \left(\frac{\partial \ (r)}{\partial} \right)_{v(r)} \qquad (10)$$

Where (r) is the electron density at the site r. Based on Eq(6), and the fact that the local softness should be integrated to give the global softness, then

$$S = \int s(r) \, dr \qquad (11)$$

The local sofness s(r) can be identified as

$$s(r) = \left(\frac{\partial}{\partial N} \right)_{v(r)} * \left(\frac{\partial N}{\partial} \right)_{v(r)} = f(r)*S \qquad (12)$$

where f(r) is the Fukui function, the intramolecular reactivity index introduced by Parr and Yang. Beacuse s(r) is obtained by multiplying f(r) with the softness S, then s(r) contains information about the intramolecular reactivity, as well as the intermolecular reactivity. Consequently, we used the local softness to compare the reactivity of each site of the two systems, that is, clean Pt surfaces and a modified surface with metallic ad-atoms. Because of the discontinuity in the derivative at the N-value of Eq. (12), we used two definitions for Fukui Function,

$$f^+(r) = \left(\frac{\partial \rho(r)}{\partial N} \right)^+_{v(r)} \quad \text{(derivative as N increases from } N_0 \rightarrow N_0 + \text{)} \quad (13)$$

for a nucleophylic attack, and

$$f^-(r) = \left(\frac{\partial \rho(r)}{\partial N} \right)^-_{v(r)} \quad \text{(derivative as N increases from } N_0 \rightarrow N_0 - \text{)} \quad (14)$$

for an electrophilic attack. In a finite difference approximation, these indices can be written as

$$f^+(r) = \rho_{N+1}(r) - \rho_N(r) \quad (15)$$

$$f^-(r) = \rho_N(r) - \rho_{N-1}(r)$$

Where $\rho_N(r)$ is the electronic –density function of the atomic or molecular anion (M=N+1) or cation (M=N-1) calculated at the geometry of the neutral system (M=N). Because we are interested in the reactivity of the atomic sites, we have considered the numbers obtained by approximate integrations of the Fukui function over atomic regions [30] (these numbers are called condensed Fukui functions). The Mulliken population analysis (MPA) scheme was used to define the atomic region.

The condensed Fukui functions are denoted as

$$f_k^+ = q_k(N+1) - q_k(N)$$

$$(16)$$

$$f_k^- = q_k(N) - q_k(N-1)$$

Where $q_k(M)$ is the atomic electron population at atom k for either the neutral system (M=N), the cation (M=N-1), or the anion M=(N+1) . Consequently, the local softness can be represented as

$$s_k^+ = f_k^+ * S \qquad (17)$$

for a nucleophilic attack, and

$$s_k^- = f_k^- * S \qquad (18)$$

for a electrophylic attack.

3-RESULTS

Stability of Pt(100)$_{25}$/Ni$_9$ and Pt(111)$_{25}$/Ni$_{10}$ structures

As a first step towards modelling a Ni covered Pt(100) and Pt(111) surface, the most favourable binding sites for a Ni atoms on Pt surfaces were determined. At each site the distance Ni-surface was optimised maintaining fixed the Pt-Pt distance in the cluster.

It was found that Ni atoms are bonded more strongly to the hollow site in Pt(100) (-3.77 eV) and hollow(3-3) in Pt(111) (-3.60 eV) surface, the equilibrium distance is equal to 0.16 nm. and 0.189 nm, respectively, as shown in Tables 1 and 2.

For comparing, Mulliken population analysis of Ni atom on Pt surface at different adsorption sites is listed in Table 3. One can see that Ni atoms are positive charged, which implies that the electron transfer occurs from Ni to Pt surface.The hollow and the hollow(3-3) sites correspond to the least electron transfer , whereas the on top sites correspond to the most one. The numbers between parenthesis in Table 3 indicate atoms involved in the interaction, taken as reference figures 2 and 3.

Our calculation also reveals that in the on top site, the electron transfer mainly occurs from Ni to Pt surface atom. But in the bridge and threefold sites, the electron transfer occurs from the two, three and four neighboring surface Pt atoms, respectively, Table 3.

The overlap population is a measure of the shared electronic density between two atoms. A large positive value indicates the atoms in question are bonded, a negative value indicates the atoms are in an anti-bonded state.

The overlap population analysis allows to understand the greater Ni atom binding energy on a face (100) than in one (111). This is due tothe fact that atom Ni interacts with four surface atoms located at a (100) plane, while at a (111) plane the interaction is through just three atoms.

Negative values for the overlap population are observed in the hollow and holllow (3-3) sites in (6-5) interaction between nickel atom and platinum atom pertaining to the inferior layer cluster, the values are -0,045 and -0,007, respectively, they indicate an anti-bonded state (Table 3).

Once determined the equilibrium position of Ni atom on Pt surfaces a Ni monolayer was deposited on both platinum surfaces, obtaining two bimetallic structures: Pt $(100)_{25}Ni_9$ and Pt $(111)_{25}Ni_{10,}$ Figure 4.

Relaxation has been allowed to Ni monolayer maintaining fixed the substrate geometry and optimizing the vertical distance between substrate-adsorbate (d_{S-A}) and nickel-nickel distance atoms (d_{Ni-Ni}) in the monolayer.

In Table 4 we can see that the distance of monolayer from platinum surface (d_{S-A}) is the largest for the adsorption on the more compact surface. In both cases the equilibrium distance (d_{S-A}) is considerably shorter than the distance between lattice planes (average distance: ($d_{Pt-Pt}+d_{Ni-Ni}$)/2). These results indicate an extraordinary strong perpendicular relaxation of adsorbate on both crystalline faces of the platinum surface.

In the lateral relaxation the distance between Ni atoms in the monolayer is greater with respect to the Ni lattice constant (Ni-Ni=0.25 nm) for both faces with values 0.290 nm and 0,268 nm for Pt (100) and Pt (111), respectively (Table 4). The resulting monolayer in both

surfaces is slightly distorted by the proper Pt substrate structure, i.e., the Ni monolayer keeps the lattice constant of the substrate. These results agree with our previous studies on this system using semiempirical methods [31].

The binding energy at the minimun for bimetallic structures Pt $(100)_{25}Ni_9$ and Pt (111) $_{25}Ni_{10}$. were used to calculate E upd according to Eq. (5) and the values are reported in the Table 5. According to our definition when Eupd is negative implies that the E $_{S-Mads}$ is greater than E $_{M-Mads}$ and then the phenomenon UPD is favored, while the opposite would predict overpotential deposition (OPD). Thus, the present results indicate that from a purely energetic view point UPD does not ocurre for these systems.

Calculations in a vacuum show that expanded monolayers are more unstable than bulk methal face consequently this can be one of the reasons for which upd is not favored.

Speculating on the posibility of the formation of an incomplete monolayer before the bulk deposition , as it happens in Pt(110), we are interested in to analyzing the reactivity of Pt/Ni bimetallic systems.

Reactivity of Pt(100)$_{25}$/Ni$_9$ and Pt(111)$_{25}$/Ni$_{10}$ structures

HOMO´s energy of a finite cluster model can directly be related with the work function of the extended system [24]. Table 6 shows the HOMO energy levels of the four systems: Pt(100)$_{25}$, Pt(111)$_{25}$, Pt(100)$_{25}$Ni$_9$ and Pt(111)$_{25}$Ni$_{10}$.

According to the HOMO energy values the clean Pt (100) 25 surfaces is more stable than the clean Pt (111) 25 surface. The n45ckel monolayer adsorption destabilize the HOMO level of both surface in 0.55 eV for Pt(100)$_{25}$Ni$_9$ and 0.44 eV for Pt(111)$_{25}$Ni$_{10}$. This means that the modified surfaces are more reactive that the clean surfaces.

Table 7 shows the values of the softness of the four systems. The softness of the surface modified increases being the Pt(111)$_{25}$Ni$_9$ the more reactive one.

The local softness values (s$^+$ y s$^-$) are plotted in Figures 5 a, b respectively, against each atom of the first layer (16 atoms) of Pt(100)$_{25}$ ad Pt(111)$_{25}$ clusters.

The local softness allows to identify the most active sites in the surface. According to Fig. 4 the greater reactivity of cluster Pt $(111)_{25}$ is located in the center. We can observe that the central atoms, 2 ,11 and 12 have the greatest values of local softness and these atoms define the hollow (3-3) site, therefore we can assign the greater activity to that site. Nevertheless, atoms near these central atoms present great values of local softness (2 and 9 atoms), consequently a zone of greater reactivity could be identified. The presence of active sites or active zone (group of atoms) favours the formation of island atoms onto this surface. This would allow to speculate with the possible formation of nickel islands on platinum surfaces before de Ni bulk deposition.

The Ni monolayer adsorption increase the local softness in the more active site and zone on Pt$(111)_{25.}$

The clean Pt$(100)_{25}$ surface present a centralized concentration of the reactivity and when it is deposited the monolayer of nickel is observed an increase in the local softness for 1, 2, 3 and 4 central atoms. These atoms define the hollow site in the surface consequently this site could be identified as the most active site.

4-CONCLUSIONS

We have investigated the stability and reactivity of Pt(100) and Pt(111) surfaces modified by nickel UPD monolayer deposition using the binding energy calculation of bimetallic structures versus the cohesion energy of the bulk adsorbate to quantify the underpotential shift (Eupd) and to determine the stability of the bimetallic systems. The reactivity of the clean and modified surface was analized by energy levels of the highest occupied molecular orbital (HOMO), softness and local softness. All our calculations were made using hybrid B3LYP density functional theory method.

According to the above-reported calculations we concluded that the stability of Pt$(100)_{25}$Ni$_9$ and Pt$(111)_{25}$Ni$_{10}$ bimetallic structures cannot be explained by the metal- substrate excess binding energy . The instability of the bimetallic systems can be related to the distorted

nickel monolayer adsorbed . Our results are not conclusive in this point because the applied model has not considered the presence of adsorption anion and solvent effects.

The reactivity of the clean Pt(100) and Pt(111) surfaces increases with the nickel monolayer adsorbed . We foud that the active sites and active zones are located in the centre of the cluster which favors the formation of island of atoms onto these surfaces.

Comparing the reactivity of the clean surfaces, the (111) face is more reactive than the (100) face. The modification of the surfaces by adsorbed monolayer reactivates both surfaces but the (111) face is the one that presents greater reactivity.

5-REFERENCES

1-Adzic R R (1984) Advances in Electrochemistry and Electrochemical Engineering, Ed. H. Gerischer (New York, John Wiley Interscience) Vol 13, p. 159.

2-Trasatti S (1976), Advances in Electrochemistry and Electrochemical Engineering, Eds. H Gerisher and C Tobias (New York, John Wiley Interscience) Vol. 10, p.213.

3-Kolb D M (1978) Advances in Electrochemistry and Electrochemical engineering, Eds. H Gerisher and C Tobias (New York: John Wiley Interscience) vol.11, p.125.

4-Szabó S, (1991) Int. Rev. , Phys. Chem. 10 (2), 207.

5-Aramata A. (1997), Modern aspect of electrochemistry, Eds. J O M Bockris, R E White

6-Leiva E P M (1993), J. Electroanal. Chem. 44,47.

7- Herrero E., Buller L J, Abruña H.D, (2001), Chem. Rev. 101, 1897.

8-El-Shafei A A, J. Electroanal. Chem. 447(1998)81.

9-Franaszczuck K, Sobkowski J, Surf. Sci. 204(1998)530.

10-Bojkov H R, Tzvetkova H R, Rashkov S, Bul. Bull of Electrochem. 7(1991)578.

11-Kania S., Holze R, Surf. Sci. 408(1998)252.

12-Obradovic M D, Grgur B N, Vracar L M, International Society of Electrochemistry, 55 annual meeting, Thessaloniki,2004.

13-Chatenet M, Faure R, Soldo-Olivier Y, J. Electroanal. Chem., 589(2005)275.

14Gaussian 03, Revision C.02, M. J. Frisch, G. W. Trucks, H. B. Schlegel, G. E. Scuseria, M. A. Robb, J. R. Cheeseman, J. A. Montgomery, Jr., T. Vreven, K. N. Kudin, J. C. Burant, J. M. Millam, S. S. Iyengar, J. Tomasi, V. Barone, B. Mennucci, M. Cossi, G. Scalmani, N. Rega, G. A. Petersson, H. Nakatsuji, M. Hada, M. Ehara, K. Toyota, R. Fukuda, J. Hasegawa, M. Ishida, T. Nakajima, Y. Honda, O. Kitao, H. Nakai, M. Klene, X. Li, J. E. Knox, H. P. Hratchian, J. B. Cross, V. Bakken, C. Adamo, J. Jaramillo, R. Gomperts, R. E. Stratmann, O. Yazyev, A. J. Austin, R. Cammi, C. Pomelli, J. W. Ochterski, P. Y. Ayala, K. Morokuma, G. A. Voth, P. Salvador, J. J. Dannenberg, V. G. Zakrzewski, S. Dapprich, A. D. Daniels, M. C. Strain, O. Farkas, D. K. Malick, A. D. Rabuck, K. Raghavachari, J. B. Foresman, J. V. Ortiz, Q. Cui, A. G. Baboul, S. Clifford, J. Cioslowski, B. B. Stefanov, G. Liu, A. Liashenko, P. Piskorz, I. Komaromi, R. L. Martin, D. J. Fox, T. Keith, M. A. Al-Laham, C. Y. Peng, A. Nanayakkara, M. Challacombe, P. M. W. Gill, B. Johnson, W. Chen, M. W. Wong, C. Gonzalez, and J. A. Pople, Gaussian, Inc., Wallingford CT, 2004.

15-Becke A D, J. Chem. Phys. 98(1993)5648.

16-Lee C, Yang W, Parr R G, Phys. Rev. B 37(1989)785.

17-Hay P J, Wadt W R, J. Chem. Phys 82(1985)270.

18-Lide R D (ED), Handbook of Chemistry and Physiscs, 72nd ed, CRC Press, West Palm Beach, Fl., (1991).

19-Szabó S, Intern. Rev. Phys. Chem. Vol 10 (1991)207.

20-Sanderson R T, Polar Covalence Academic Press, New York (1983).

21-Pearson R G, J. Am. Chem. Soc. 105(1983)7512.

22- Pearson R G, J.Chem. Educ. 64(1987)561.

23-Chattaraj P K, Lee H, Parr R G, J. Am. Chem. Soc. 113(1985)1991.

24-Yang W, Mortier W J, Proc. Natl. Acad. Sci. USA 82(1985)6723.

25-Parr R G, Pearson R J, J. Am. Chem. Soc. 105(1983)7512.

26-Parr R G, Yang W, Density Functional Theory of Atoms and Molecules, Oxford University Press, New York, (1989).
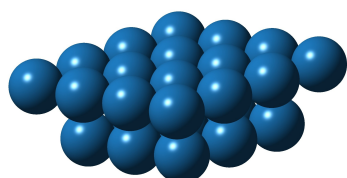
27-Ghosh S K, Berkowitz M, J. Am. Chem. Phys. 83(1985)2976.

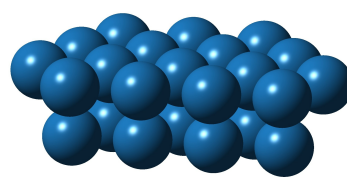28-Berkpwitz M, Parr R G, Chem Phys J. 88(1988)2554.

29-Parr G R, Yang W, J. Am. Chem. Soc. 106(1984)4049.

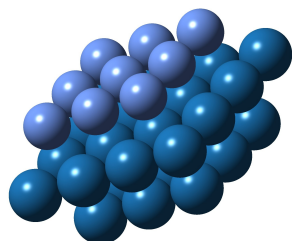30-Yang W, Mortier W J, J. Am. Chem. Soc. 108(1986)5708

31- López M B, Estiú G L, Castro E. A., Arvía A J, (1990) J. Mol. Structure (THEOCHEM) 210, 353.
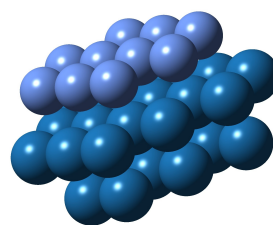
(a)

(b)

(c)

(d)

Figure 1- Clusters used in the calculations: a)Pt(100)$_{25}$, b)Pt(111)$_{25}$, c)Pt(100)$_{25}$Ni$_9$, d)Pt(111)$_{25}$Ni$_{10}$
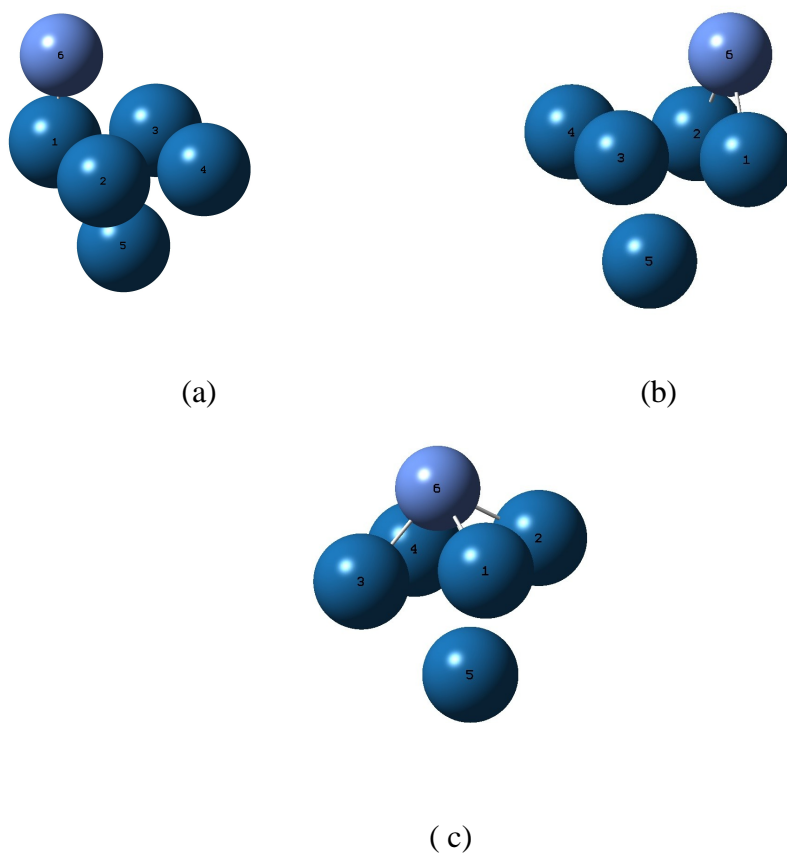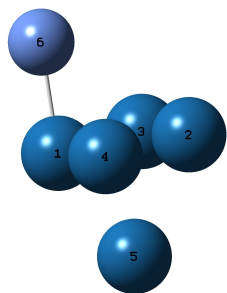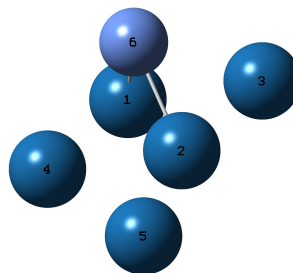
(a)

(b)

(c)

Figure 2. Different adsorption sites on Pt(100) surface: a) On top, b)Bridge, c)Hollow.
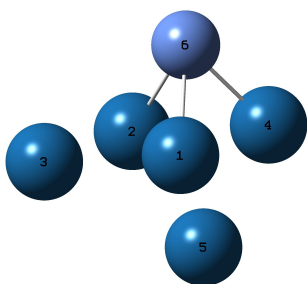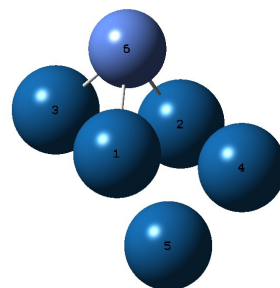
(a)

(b)

(c)

(d)

Figure 3-Different adsorption sites on the Pt(111) surface: a)on top, b)bridge,
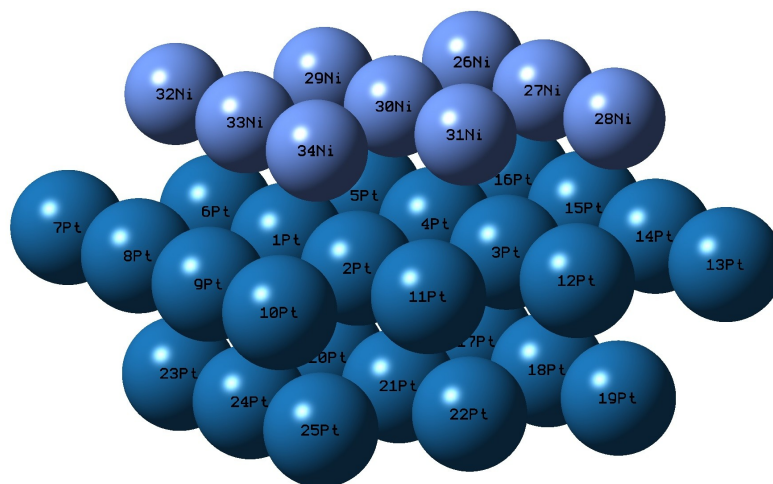 c) hollow(3-1), d)hollow (3-3).

Figure 4 a) Structure Pt(100)$_{25}$Ni$_9$

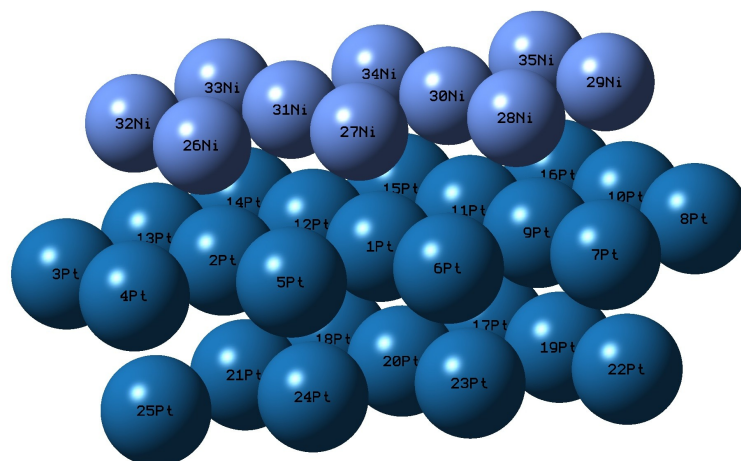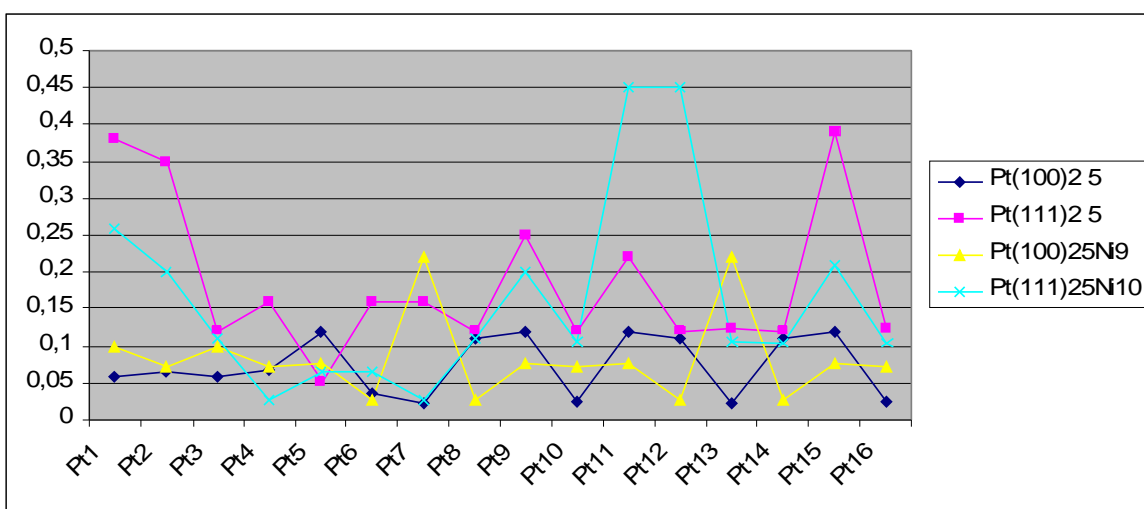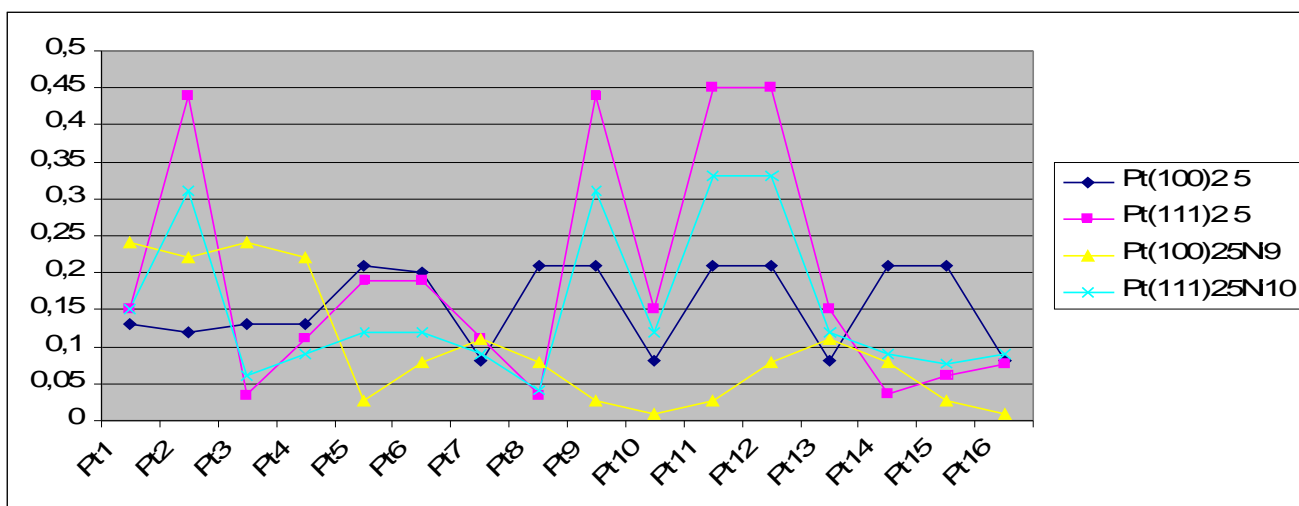Figure 4 b)Structure Pt(111)$_{25}$Ni$_{10}$

a)

b)

Figure 5-Local softness: a) for electrophilic reaction, and b) for nucleophilic reaction

Table 1-Binding energy values (BE, eV) and equilibrium distance (d, nm) for the adsorption

of Ni atoms on different Pt(100)$_{25}$ cluster surface sites.

Site	BE (eV)	d (nm)
On Top	-1.62	0.230
Bridge	-2.90	0.190
Hollow	-3.77	0.160

Table 2- Binding energy values (BE, eV) and equilibrium distance (d, nm) for the

adsorption of Ni atoms on different Pt(111)$_{25}$ cluster surface sites.

Site	BE (eV)	d (nm)
On Top	-2.34	0.232
Bridge	-3.25	0.194
Hollow(3-3)	-3.60	0.186
Hollow (3-1)	-3.35	0.190

Sites		Net Charge of Ni atom	Overlap population/bond	
Pt(100)				
	On-Top	0.53	(6-1)	0.21
	Bridge	0.49	(6-1)	1.6
			(6-2)	1.6
	Hollow	0.15	(6-1)	1.28
			(6-2)	1.28
			(6-3)	1.28
			(6-4)	1.28
			(6-5)	-0.045
Pt(111)				
	On-Top	0.55	(6-1)	0.27
	Bridge	0.39	(6-1)	0.20
			(6-2)	0.20
	Hollow (3-3)	0.36	(6-1)	0.20
			(6-2)	0.20
			(6-3)	0.23
	Hollow (3-1)	0.41	(6-1)	0.16
			(6-2)	0.16
			(6-3)	0.15
			(6-4)	0.15
			(6-5)	– 0.007

Table 3-Mulliken population analysis of Ni on different adsorption sites (numbers

between parenthesis are related to Figures 2 and 3)

Table 4-Equilibrium distances after the relaxation process: $d_{(Ni-Ni)}$ (nm) is the distance between nickel atoms, $d_{(A-S)}$ (nm) is the perpendicular distance between adsorbate-substrate.

System	$d_{(Ni-Ni)}$ (nm)	$d_{(A-S)}$ (nm)
Pt(100)Ni	0.290	0.160
Pt(111)Ni	0.268	0.193

Table 5- Energies that contribute to theoretical estimation of the underpotential shifts:

E_{S-Mad} (eV), binding energy between substrate (S) and metallic monocapa adsorbed (Mad),

) E_{M-Mad} (eV), binding energy between deposited metal atom (Mad) on a surface of its own

kind (M).   Eupd (eV), is the underpotential shifts.

System	E_{S-Mad} (eV)	E_{M-Mad} (eV)	Eupd (eV)
(100)	-2.52	-2.98	0.46
(111)	-2.39	-2.75	0.36

Table 6- Energy levels of the highest occupied molecular orbital (HOMO, eV) of the

systems

System	HOMO (eV)
Pt(100)	-5.90
Pt(100)Ni	-5.35
Pt(111)	-5.69
Pt(111)Ni	-5.25

Table 7-Softness of the systems

System	Softness
Pt(100)	3.33
Pt(100)Ni	4.08
Pt(111)	2.66
Pt(111)Ni	3.45